This is the accepted manuscript made available via CHORUS. The article has been published as:

Self-similar rupture of thin free films of power-law fluids

Sumeet Suresh Thete, Christopher Anthony, Osman A. Basaran, and Pankaj Doshi

Phys. Rev. E **92**, 023014 — Published 12 August 2015

DOI: 10.1103/PhysRevE.92.023014

Self-similar rupture of thin free films of power law fluids

Sumeet Suresh Thete, Christopher Anthony, and Osman A. Basaran
School of Chemical Engineering, Purdue University, West Lafayette, IN 47906, USA

Pankaj Doshi
Chemical Engineering and Process Development, National Chemical Laboratory, Pune, India

Rupture of a thin free film of a power law fluid under the competing influences of destabilizing van der Waals pressure and stabilizing surface tension pressure is analyzed. In such a fluid, viscosity decreases with deformation rate raised to the $n-1$ power where $0 < n \leq 1$ ($n = 1$ for a Newtonian fluid). When $6/7 < n \leq 1$, film rupture occurs under a balance between van der Waals pressure, inertial stress, and viscous stress. When $n < 6/7$, however, the dominant balance changes: viscous stress becomes negligible and the film ruptures under the competition between van der Waals pressure, inertial stress, and surface tension pressure.

I. INTRODUCTION

Dynamics of thin films are important in technology and nature [1, 2]. Both free films, or sheets, where the film has two free surfaces (Fig. 1) [3–7], and supported films, where the film lies on a solid substrate and has a single free surface [8, 9], are of interest. In the former, the intermolecular van der Waals attraction between the molecules in the film and, in the latter, the van der Waals attraction between the molecules in the film and the solid can cause the film to rupture despite the stabilizing influence of surface tension. The van der Waals attraction in free films is the key effect by which foams collapse and two drops coalesce [10–12]. Similarly, van der Waals attraction in supported films is central to film rupture and formation of dry spots in coating and heat transfer applications [13–17].

Study of dynamics of free films has been of interest since at least Ref. [18]. Recent work has focused on the self-similar dynamics and finite time singularities that arise during film rupture [6]. In this paper, the nonlinear dynamics leading to the rupture of a thin free film of a power law fluid is analyzed. If the two flat surfaces of a thin liquid film of constant thickness $2h_0$ are subjected to static shape deformations that are symmetric about the midplane of the unperturbed sheet that lies in the xz-plane and the perturbations are translationally-symmetric in the x-direction so that the shape of one of the two interfaces between the liquid film and the surrounding gas can be represented as $y = h(z)$, the pressure in a nearly flat static film is given by

$$p = \frac{A}{6\pi(2h)^3} - \sigma \frac{\partial^2 h}{\partial z^2} \tag{1}$$

where A is the Hamaker constant, σ is the surface tension, the pressure in the gas is taken as the pressure datum, and the effect of gravity is neglected on account of the film's thinness. Thus, as is well known, the van der Waals pressure (the first term) is destabilizing because it would cause flow from the neck toward the swell whereas surface tension or capillary pressure (the second term) is stabilizing because it would cause flow from the swell toward the neck. If the perturbation is a sinusoidal deformation of wavelength λ and small amplitude $\epsilon \ll 1$,

$$h = h_0 \left[1 - \epsilon \cos\left(\frac{2\pi z}{\lambda}\right)\right], \tag{2}$$

it is readily shown from a simple pressure driving force argument or a more sophisticated linear stability analysis [6] that disturbances of wavelengths exceeding a critical value $\lambda_c = 8\pi^{3/2}\sigma^{1/2}h_0^2/A^{1/2} = 8\pi^{3/2}h_0^2/d$ are unstable, where $d \equiv (A/\sigma)^{1/2}$ is the molecular lengthscale. For a continuum approach to be valid, $h_0 \gg d$. Thus, $\lambda_c \gg h_0$ and the instability is a long-wavelength one. Vaynblat et al. [6] used the long-wavelength approximation to derive a set of one-dimensional (1D) equations to analyze the thinning and rupture of thin films of Newtonian fluids and showed that the dominant physical balance is between inertial, viscous, and van der Waals stresses, while surface tension stress is negligible. These authors further showed that the film thickness h, lateral scale $z' \equiv z - z_R$, where $z = z_R$ is the lateral location where the film ruptures, and lateral velocity v vary with time remaining to rupture $\tau \equiv t_R - t$, where t_R is the time t at which the film ruptures, as $h \sim \tau^{1/3}$, $z' \sim \tau^{1/2}$, and $v \sim \tau^{-1/2}$. If, however, the film is supported on a substrate, both the dominant balance and the scaling exponents differ from the situation just discussed, as shown by [9].

Many fluids in emerging applications involving free surface flows of films, jets, and drops are non-Newtonian [19–21]. One important type of a non-Newtonian fluid is a so-called power law fluid. In contrast to a Newtonian fluid that has a constant viscosity μ_0, the viscosity μ of a power law fluid varies with deformation rate as $\mu = \mu_0|m\dot{\gamma}|^{n-1}$. Here μ_0, the zero-deformation-rate viscosity, and m^{-1}, the characteristic deformation rate, are constants, $0 < n \leq 1$ is the power law exponent ($n = 1$ corresponds to a Newtonian fluid), and $\dot{\gamma}$ is the second invariant of the rate-of-deformation tensor $\mathbf{D}$: $\dot{\gamma} = [1/2(\mathbf{D} : \mathbf{D})]^{1/2}$ and $\mathbf{D} = 1/2\left[\nabla\mathbf{v} + (\nabla\mathbf{v})^T\right]$, where $\mathbf{v}$ is the velocity. The goal of this work is to analyze the rupture of thin films of power law fluids. Of particular relevance to the present paper are theoretical studies of pinch-off of cylindrical liquid threads of power

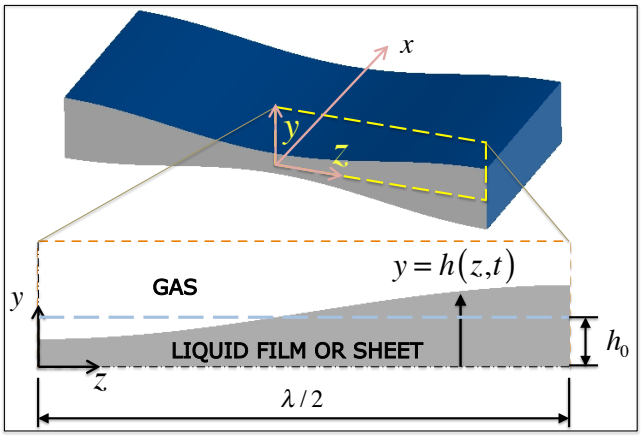

FIG. 1. A liquid film: perspective view (top) and cross-sectional view showing problem domain (bottom).

law fluids [22–25] which exhibit even richer behavior than their Newtonian counterparts [26–28]. Some of the predicted behaviors have been confirmed by recent experiments [20, 21]. A noteworthy finding of these studies is that when $1 \geq n > n_c$, where n_c is a critical value of n, liquid threads pinch-off under a balance of inertial, viscous, and surface tension forces but when $n < n_c$, a thread pinches off as if it were an inviscid fluid of zero viscosity. Motivated by this result, we investigate whether a similar change of scaling behavior can occur during rupture of thin films of power law fluids. Unfortunately, all previous attempts to study power law film rupture have involved simplifying assumptions such as neglecting inertia in both film rupture on a planar substrate [29] and that on a solid cylinder [30], or entirely omitting nonlinear effects [31].

Rupture of a thin liquid film, as in pinch-off of a liquid thread, gives rise to a finite time singularity in the governing equations. The dynamics close in time and space to the singularity are expected to be universal and hence independent of the boundary and initial conditions. The goals are to examine the self-similar evolution of the film toward the space-time singularity, determine scaling exponents governing the time evolution of film thickness and other relevant problem variables, and construct similarity profiles for the interface shapes.

The paper is organized as follows. In the next section, the transient partial differential equations (PDEs) that govern the film profile and the velocity within the film are presented. In Section III, the forms of the similarity solutions are deduced by dominant balance type arguments, and the transient PDEs are solved numerically to obtain the time evolution of the film profile and the velocity field within the film. The results from time dependent simulations are also shown in Section III to agree well with the similarity solutions. Concluding remarks are then presented in Section IV.

II. PROBLEM STATEMENT

The system is a free film of a power law fluid of initial thickness $2h_0$ and constant density ρ, as shown in Fig. 1. The film is disturbed by a laterally periodic perturbation of wavelength $\lambda \gg h_0$ (typically, $\lambda/h_0 \approx 10^5$). In this paper, only line rupture of the film is analyzed so that the instantaneous shape of the interface is described as $y = h(z,t)$. The long wavelength nature of the problem can be taken advantage of by reducing the governing Cauchy momentum and continuity equations, subject to the traction and kinematic boundary conditions at the film-ambient gas interface, to a set of 1D evolution equations for the interface shape h and lateral velocity v. It also proves convenient to render the problem statement dimensionless by using as characteristic film thickness $h_c = h_0$, lateral length scale $l_c = (48\pi h_0^3 \mu_0^2/\rho A)^{1/2}$, time scale $t_c = \rho l_c^2/\mu_0$, velocity scale $v_c = l_c/t_c$, and viscosity scale $\mu_c = \mu_0$ so that the dimensionless shape function, lateral length, time, velocity, and viscosity are given by $\tilde{h} \equiv h/h_c$, $\tilde{z} \equiv z/l_c$, $\tilde{t} \equiv t/t_c$, $\tilde{v} \equiv v/v_c$, and $\tilde{\mu} \equiv \mu/\mu_c$. The dimensionless set of 1D evolution equations governing the sheet half-thickness and lateral velocity are given by

$$\frac{\partial h}{\partial t} + \frac{\partial (hv)}{\partial z} = 0 \tag{3}$$

$$\frac{\partial v}{\partial t} + v\frac{\partial v}{\partial z} = S\frac{\partial^3 h}{\partial z^3} - \frac{\partial \left(h^{-3}\right)}{\partial z} + \frac{4}{h}\frac{\partial}{\partial z}\left(\mu h \frac{\partial v}{\partial z}\right) \tag{4}$$

where the dimensionless viscosity $\mu = |2m\ \partial v/\partial z|^{n-1}$. In these equations and henceforward, the tildes over the dimensionless variables are omitted for clarity. Also in these equations, $S \equiv \rho h_0 \sigma/\mu_0^2$ is a dimensionless parameter that equals the product of inertial and surface tension forces divided by viscous force squared. The reciprocal of S equals the square of the Ohnesorge number Oh.

III. DOMINANT BALANCES, SIMILARITY SOLUTIONS, AND NUMERICAL SIMULATIONS

A. Power law fluids of $6/7 < n \leq 1$

As the singularity (z_R, t_R) is approached, the film profile and lateral velocity are expected to be described by similarity solutions of the form

$$h(z',\tau) = \tau^{\alpha} H(\xi)\,,\ v(z',\tau) = \tau^{\gamma} U(\xi)\,,\ \xi = z'/\tau^{\beta} \tag{5}$$

where $\tau = t_R - t$ is the dimensionless time to rupture, $z' = z - z_R$ is the lateral extent of the rupture zone, and ξ is the similarity variable. Here, α, γ, and β are scaling exponents and H and U are scaling functions that are to be determined. Substitution of the similarity solutions (Eq. 5) into the 1D mass balance (Eq. 3) and enforcing that the resulting equation is independent of

time or carrying out a kinematic balance of the terms in that equation gives $\gamma - \beta = -1$. Doing the same with the 1D momentum balance (Eq. 4) or carrying out a dynamical balance of the terms in that equation reveals that the dominant balance is between the van der Waals, viscous, and inertial forces, with surface tension force being negligible, and that

$$\alpha = n/3\,, \quad \gamma = -n/2\,, \quad \beta = 1 - n/2 \tag{6}$$

With these exponents, it is readily seen that the van der Waals, viscous, and inertial terms in the 1D momentum equation all blow up as $\tau^{-n/2-1}$ whereas the surface tension term blows up as $\tau^{11n/6-3}$. From the viscosity relation, it follows that $\mu \sim \tau^{1-n} \sim h^{3(1-n)/n}$. In the Newtonian limit ($n = 1$), the scaling exponents take on the values $\alpha = 1/3$, $\gamma = -1/2$, and $\beta = 1/2$ in accord with prior work [6], and the dominant terms all blow up as $\tau^{-3/2}$ whereas the slower growing surface tension term blows up as $\tau^{-7/6}$.

The 1D evolution equations were next solved numerically [22, 24]. Figure 2 shows the results of such simulations when $n = 0.94$. The simulation results show that the variation with τ of the computed value of the minimum film thickness $h_{\min} \equiv h(z = 0, t)$ is in excellent agreement with the theoretically predicted variation $h_{\min} \sim \tau^{n/3} \equiv \tau^{0.3133\ldots}$ (Fig. 1(a)). To evaluate the lateral scale from simulation data, the variation with τ of the z-coordinate of a point located on the interface for which the film thickness equals a multiple of $h_{\min}$ is monitored. Once again, the computed variation of z' with τ is seen to be in excellent accord with the theoretical prediction of $z' \sim \tau^{0.53}$ (Fig. 1(b)). The simulations further show that the variation with τ of the lateral velocity v' calculated at z' is in excellent agreement with the theoretical prediction of $v' \sim \tau^{-0.47}$ (Fig. 1(c)). Finally, evaluating the variation with τ of the viscosity μ' at z' but then recasting this variation as μ' versus $h_{\min}$ demonstrates that the computed prediction accords well with the theoretical prediction of $\mu' \sim h_{\min}^{3(1-n)/n} \equiv h_{\min}^{0.1914\ldots}$ (Fig. 1(d)).

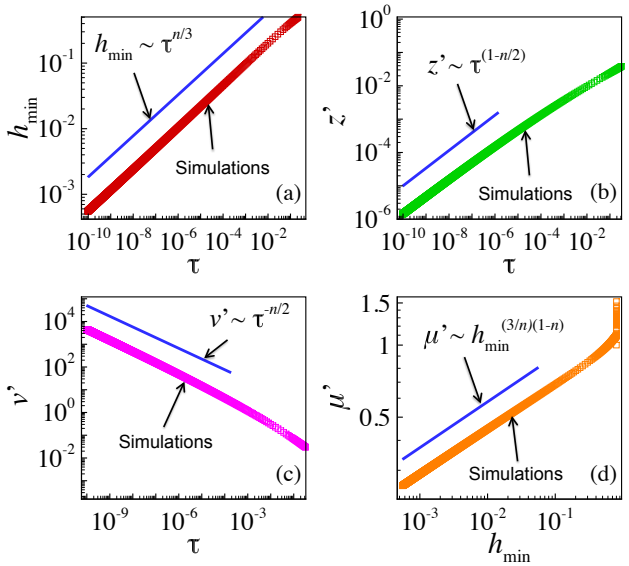

FIG. 2. Scaling behaviors when $n = 0.94$ of (a) minimum film thickness $h_{\min}$, (b) lateral length scale z', (c) lateral velocity v', and (d) viscosity μ'. The straight lines are the theoretical predictions and data points show simulation results. In this figure and the next, $S = 3/(2\pi^2)$ and $m = 1$.

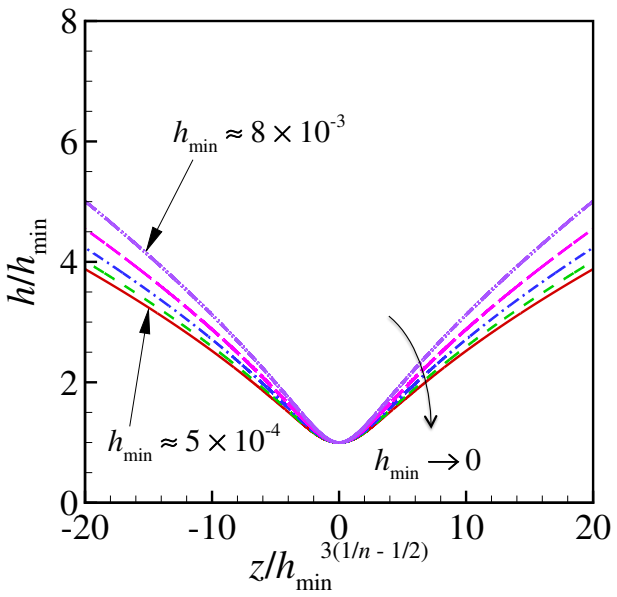

FIG. 3. Transient film profiles scaled by minimum film thickness as a function of scaled lateral coordinate show approach to the similarity profile as $h_{\min} \to 0$. For each profile depicted at successively smaller values of $h_{\min}$, $h_{\min}$ is roughly half that of the previously shown profile. Here, $n = 0.94$.

The scaling exponents in Eq. 6 can be used to collapse transient film profiles obtained from simulations. Since $h = \tau^{n/3} H(\xi)$ and $\xi = (z - z_R)/\tau^{1-n/2}$ (with $z_R = 0$), Fig. 3 shows the variation of the scaled interface profile $h/h_{\min}$ with the scaled lateral coordinate $z/h_{\min}^{3(1/n-1/2)}$. Figure 3 demonstrates that the computed scaled shapes tend to a similarity profile as $h_{\min} \to 0$.

Examining the variation with τ of the four forces as a function of the power law exponent n reveals that when $n = 6/7$ all the terms in the 1D momentum equation blow up as $\tau^{-10/7}$. Therefore, surface tension force is negligible and the scaling exponents have the values given in Eq. 6 only when $6/7 < n \leq 1$.

B. Power law fluids of $n < 6/7$

Because the rate at which viscosity falls with decreasing film thickness rises as n decreases, it is anticipated that viscous force may become less important compared to the other three forces when $n < 6/7$. In anticipa-

tion of the new balance of forces, the governing equations are rescaled using as a new characteristic length scale $l_c = (48\pi h_0^4\sigma/A)^{1/2}$ and as a new characteristic time $t_c = (\rho l_c^4/\sigma h_0)^{1/2}$. The new nondimensionalization leaves the 1D mass balance and the viscosity relation unchanged but modifies the 1D momentum balance such that the surface tension term is now multiplied by one but the viscous term by Oh.

Carrying out the kinematical and the dynamical balance arguments once again reveals that the scaling exponents when $n < 6/7$ are given by

$$\alpha = 2/7\,, \quad \gamma = -3/7\,, \quad \beta = 4/7 \tag{7}$$

With these exponents, it is readily seen that the van der Waals, surface tension, and inertial terms in the 1D momentum equation all blow up as $\tau^{-10/7}$ whereas the viscous term blows up as $\tau^{-n-4/7} = \tau^{-10/7+(6/7-n)}$. From the viscosity relation, it follows that $\mu \sim \tau^{1-n} \sim h^{7(1-n)/2}$, as when $n > 6/7$. The 1D evolution equations were then solved numerically once again. Figure 4 shows the results of such simulations when $n = 0.6$. The simulation results show that the variation with τ of the computed value of the minimum film thickness $h_{\min}$, the lateral extent z' of the rupture region, the lateral velocity v', and viscosity μ' are in excellent agreement with the theoretical predictions (Eq. 7). The scaling exponents reported in Eq. 7 are also used to collapse transient film profiles obtained from simulations. Since $h = \tau^{2/7}H(\xi)$ and $\xi = (z - z_R)/\tau^{4/7}$ (with $z_R = 0$), Fig. 5 shows the variation of the scaled interface profile $h/h_{\min}$ with the scaled lateral coordinate $z/h_{\min}^2$. Figure 5 demonstrates that the computed shapes tend to a similarity profile as $h_{\min} \to 0$.

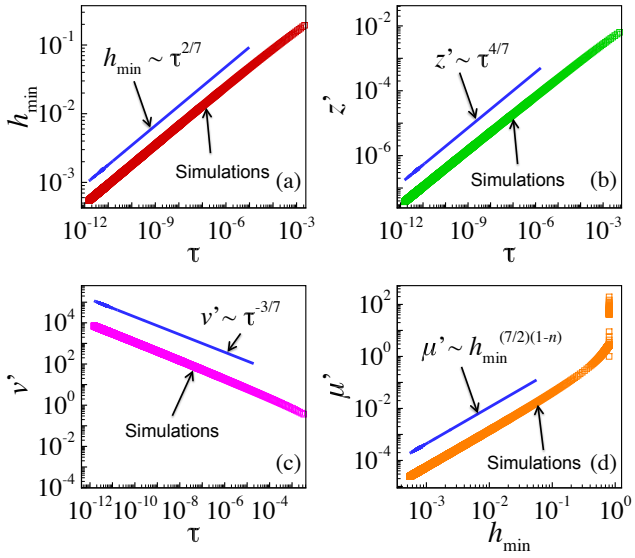

FIG. 4. Scaling behaviors when $n = 0.60$ of (a) minimum film thickness $h_{\min}$, (b) lateral length scale z', (c) lateral velocity v', and (d) viscosity μ'. The straight lines are the theoretical predictions and data points show simulation results. In this figure and the next, $Oh = \sqrt{(2/3)}\pi$ and $m = 1$.

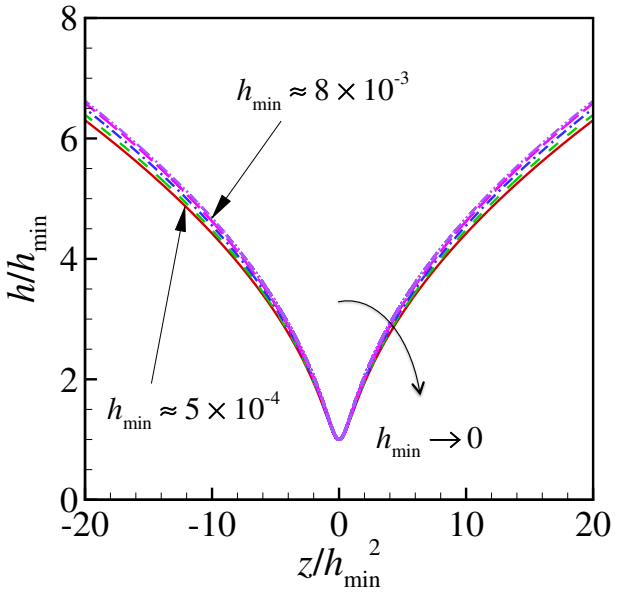

FIG. 5. Transient film profiles scaled by minimum film thickness as a function of scaled lateral coordinate show approach to the similarity profile as $h_{\min} \to 0$. For each profile depicted at successively smaller values of $h_{\min}$, $h_{\min}$ is roughly half that of the previously shown profile. Here, $n = 0.60$.

IV. CONCLUSIONS

At the onset of the initial instability, the aspect ratio of the film $\epsilon \equiv h_0/l_0 < d/h_0 \ll 1$, where h_0 and l_0 are the initial film thickness and the initial lateral extent of the film, and d is the molecular length scale. However, given the exponents of the characteristic length scales obtained in this paper, the local slope of the interface diverges as rupture is approached. Therefore, the long wavelength assumption on which the governing equations 3 and 4 are based may potentially be violated prior to film rupture. It will now be demonstrated, however, that molecular length scales are reached first before the long wavelength assumption fails. In terms of dimensional variables, the continuum approximation fails when the dimensional value of half the minimum film thickness $h_{\min}(t) \approx d$.

When $n < 6/7$, the film thickness varies as $h \sim \tau^{2/7}$ and the lateral length scale as $l \sim \tau^{4/7}$. Therefore, the aspect ratio of the film varies as $\epsilon\tau^{-2/7}$. The aspect ratio reaches order unity when the film thickness and the lateral length scale are of order $\epsilon h_0 < d$. Thus, in this case, the continuum approximation breaks down before the long wavelength approximation.

When $6/7 < n \leq 1$, the film thickness varies as $h \sim \tau^{n/3}$ and the lateral length scale as $l \sim \tau^{1-n/2}$.

Therefore, the aspect ratio of the film varies as $\epsilon\tau^{5n/6-1}$. The aspect ratio reaches order unity when the film thickness and the lateral length scale are of order $h_0\epsilon^{2n/(6-5n)}$. When $n = 1$ (Newtonian fluid), the film aspect ratio becomes order one when both length scales are of order $d^2/h_0 \ll d$. When $n = 6/7 + \delta$ where $\delta \ll 1$, the film aspect ratio becomes order one when both length scales are of order $d(d/h_0)^{49\delta/12} < d\epsilon^{49\delta/12} < d$. Thus, regardless of the value of n, the continuum approximation breaks down before the long wavelength approximation.

The results reported here can be extended to analyze the case of so-called point rupture where the scaling exponents turn out to be identical to ones reported here [32]. Furthermore, in both cases, the similarity solutions $H(\xi)$ and $U(\xi)$ can be determined directly by solving a set of ordinary differential equations in similarity space [32]. Aside from their intrinsic theoretical value, improved understanding of thread pinch-off [22–25] and film rupture singularities (this paper), and associated self-similar behavior during thinning, also hold the potential for creating improved cutoff schemes in large-scale simulations of drop breakup and coalescence [11, 19] involving power law fluids.

V. ACKNOWLEDGMENTS

The authors thank the Basic Energy Sciences (BES) program of the United States Department of Energy (DE-FG02-96ER14641) and the Donors of the American Chemical Society Petroleum Research Fund for financial support.

[1] G. F. Teletzke, H. Ted Davis, and L. E. Scriven, Chemical Engineering Communications **55**, 41 (1987).
[2] A. Oron, S. H. Davis, and S. G. Bankoff, Reviews of Modern Physics **69**, 931 (1997).
[3] M. Prévost and D. Gallez, The Journal of Chemical Physics **84**, 4043 (1986).
[4] T. Erneux and S. H. Davis, Physics of Fluids A: Fluid Dynamics (1989-1993) **5**, 1117 (1993).
[5] M. Ida and M. Miksis, Applied Mathematics Letters **9**, 35 (1996).
[6] D. Vaynblat, J. R. Lister, and T. P. Witelski, Physics of Fluids **13**, 1130 (2001).
[7] J. Burton and P. Taborek, Physics of Fluids **19**, 102109 (2007).
[8] J. P. Burelbach, S. G. Bankoff, and S. H. Davis, Journal of Fluid Mechanics **195**, 463 (1988).
[9] W. W. Zhang and J. R. Lister, Physics of Fluids **11**, 2454 (1999).
[10] A. Chesters, Chemical Engineering Research & Design **69**, 259 (1991).
[11] Y. Yoon, F. Baldessari, H. D. Ceniceros, and L. G. Leal, Physics of Fluids **19**, 102102 (2007).
[12] S. Cohen-Addad, R. Höhler, and O. Pitois, Annual Review of Fluid Mechanics **45**, 241 (2013).
[13] S. F. Kistler and L. E. Scriven, International Journal for Numerical Methods in Fluids **4**, 207 (1984).
[14] M. Elbaum and S. Lipson, Physical Review Letters **72**, 3562 (1994).
[15] M. Elbaum and S. Lipson, Israel Journal of Chemistry **35**, 27 (1995).
[16] S. J. VanHook, M. F. Schatz, W. D. McCormick, J. Swift, and H. L. Swinney, Physical Review Letters **75**, 4397 (1995).
[17] M. Bowen and B. Tilley, Physics of Fluids **24**, 032106 (2012).
[18] G. I. Taylor, Proceedings of the Royal Society of London. Series A. Mathematical and Physical Sciences **253**, 313 (1959).
[19] O. A. Basaran, H. Gao, and P. P. Bhat, Annual Review of Fluid Mechanics **45**, 85 (2013).
[20] J. R. Savage, M. Caggioni, P. T. Spicer, and I. Cohen, Soft Matter **6**, 892 (2010).
[21] F. Huisman, S. Friedman, and P. Taborek, Soft Matter **8**, 6767 (2012).
[22] P. Doshi, R. Suryo, O. E. Yildirim, G. H. McKinley, and O. A. Basaran, Journal of non-Newtonian Fluid Mechanics **113**, 1 (2003).
[23] P. Doshi and O. A. Basaran, Physics of Fluids **16** (2004).
[24] R. Suryo and O. A. Basaran, Journal of non-Newtonian Fluid Mechanics **138**, 134 (2006).
[25] M. Renardy, Journal of non-Newtonian Fluid Mechanics **104**, 65 (2002).
[26] J. Eggers, Physical Review Letters **71**, 3458 (1993).
[27] D. T. Papageorgiou, Physics of Fluids **7**, 1529 (1995).
[28] R. F. Day, E. J. Hinch, and J. R. Lister, Physical Review Letters **80**, 704 (1998).
[29] C.-C. Hwang and S.-H. Chang, Journal of Applied Physics **74**, 2965 (1993).
[30] R. S. R. Gorla, Journal of Applied Mechanics **68**, 294 (2001).
[31] A. N. Sathyagal and G. Narsimhan, Chemical Engineering Communications **111**, 161 (1992).
[32] S. S. Thete, *Singularities in free surface flows*, Ph.D. thesis, Purdue University (2015).